CMS Draft Analysis Note

The content of this note is intended for CMS internal use and distribution only

2009/05/30
Archive Id:
Archive Date:

Search for Supersymmetry with Trimuons

V. Zhukov, M. Niegel, W. de Boer, A. Cakir, D. Troendle, and E. Ziebarth
Institut für Experimentelle Kernphysik, University of Karlsruhe

Abstract

The discovery reach of CMS for the SUSY trimuon final state is studied for the LHC startup scenario at $\sqrt{s}$=10 TeV. The trimuon signature appears in leptonic decays of charginos and neutralinos and potentially has only a small Standard Model background in comparison with other SUSY searches. This allows to perform SUSY searches without requiring cuts on missing transverse energy or the number of jets and their energies, which are prone to large uncertainties during the first year of operation. The trimuon signal can be observed at an integrated luminosity below 1 fb^{-1} in the low mass SUSY region using the SM background estimation from experimental data.

Contents

1 Introduction

Neutralinos (χ^0) and charginos ($\chi^\pm$) are the main source of prompt isolated muons in SUSY production. The gauginos can be produced directly $pp \to \chi_2^0 + \chi_1^\pm$ or in the decays of squarks and gluinos. Some typical Feynman diagrams are shown in Figure 1. The first case corresponds to the pure trimuon signature with some missing transverse energy (MET) from the escaping lightest superymmetric particles (LSP) and neutrino, but no hard jets are present in this case. The direct gaugino production is the dominant SUSY production channel at the Tevatron at $\sqrt{s}$=1.96 TeV, since here antiprotons are collided, so energetic antiquarks are present. Therefore, the SUSY trilepton signature has been intensively searched for at the Tevatron with negative results so far for an accumulated luminosity of $L_{acc} \sim 2$ fb^{-1}, thus excluding the low mass SUSY region [1]. At the LHC the dominant SUSY production channels are gluino $\tilde{g}$ or squarks $\tilde{q}$, if kinematically accessible. The cascade decays of gluinos and squarks result in many hard jets in addition to the MET and muons and in this respect the trimuon signature is not much different from other SUSY searches with one or two muons.

The prospects for direct neutralino-chargino production at LHC have been studied by CMS for operation at 14 TeV and an accumulated luminosity $L_{acc} > 10$ fb^{-1} [2]. Here we repeat this study for 10 TeV and simultaneously extend it by allowing hard jets in the 3l signature, so one is simultaneously sensitive to gaugino and gluino production. This yields somewhat more background, but eliminates the large systematic uncertainties originating from cuts on jet multiplicities and jet energies. The SM background will be estimated in a data driven way by using the side bands in the isolation distributions of the muons.

In the Standard Model (SM) isolated muons are mostly produced by leptonic decays of gauge bosons Z/γ, W. The larger the number of muons in the final state, the smaller the SM background. For the trimuon final state there are a few SM channels with small but not negligible cross section, which produce three or more isolated prompt muons: ZW, ZZ and WWW. The observation of the Z-peak in ZW events gives possibility to check the efficiency of the SUSY trimuons analysis.

The suppression of SM backgrounds in SUSY searches usually requires selection on MET and jets which are prone to large theoretical and instrumental systematic uncertainties, especially at the beginning of LHC operation. This makes a clean trimuon signature an attractive candidate for the early SUSY searches without suffering from the hadronic uncertainties.

This study presents an inclusive search in the SUSY trimuon final state optimized for the startup period of CMS operation at 10 TeV. The analysis is based on MC data samples produced with the full detector simulations in 2008-2009 years.

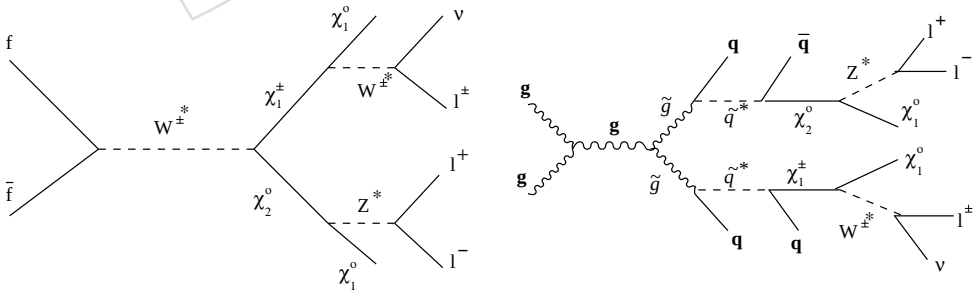

Figure 1: Typical diagrams for the trimuon production in SUSY

2 SUSY signal and Standard Model backgrounds

The trimuon final state is a generic signature for SUSY models, though different scenarios may affect the production cross section. In this study the mSUGRA model was used to simulate the signal.

The mSUGRA model is characterized by 5 parameters (m_0, $m_{1/2}$, tanβ, A_0, sgnμ) [5], where masses of neutralinos and charginos are defined by the common GUT scale mass for spin 1/2 particles, called $m_{1/2}$: $m_{\chi_1^0} \approx 0.4 \cdot m_{1/2}$, $m_{\chi_2^0} \approx \chi_1^{\pm} \approx 0.8 \cdot m_{1/2}$ (except a region near EWSB at $\mu \to 0$), and $m_{\tilde{g}} \sim 2.7 m_{1/2}$. For heavy squarks, sleptons and light gauginos ($m_0 > 100$ GeV and $m_{1/2} < 300$ GeV) the neutralino χ_2^0 decays via an off-shell Z^* with subsequent decay into muons with a typical branching ratio of 3%, whereas the chargino $\chi_1^{\pm}$ decays to muons via an off-shell W^* with a branching ratio of 11%. For low slepton masses ($m_0 \leq 100$ GeV) the charginos and neutralinos may decay directly to a sleptons-lepton pair. These two-body decays will dominate over the three-body decays discussed above, if energetically allowed. In both cases, 3- and 2-body decays the opposite sign (OS) muons have a kinematic end point in the $M_{\mu\mu}$ invariant mass distribution: $M_{max} = m_{\chi_2^0} - m_{\chi_1^0}$ for 3-body decays and $M_{max}=\sqrt{(m^2_{\chi_2^0} - m^2_{\tilde{l}})(m^2_{\tilde{l}} - m^2_{\chi_1^0})/m^2_{\tilde{l}}}$ for 2-body decays into sleptons with mass $m_{\tilde{l}}$. For heavier gauginos ($m_{1/2} > 300$ GeV) the neutralino χ_2^0 decays via on-shell Z-exchange and at even larger $m_{1/2}$ via Higgs-exchange. This limits the range of invariant mass of OS muon pairs to $M_{\mu\mu} < M_Z$.

In mSUGRA the direct production of neutralino and chargino $pp \to \chi_2^0 + \chi_1^{\pm}$ has a significant fraction only at large m_0 where the squarks become too heavy. Figure 2 shows the total cross sections and fractional trimuon final state at 10 TeV in the m_0-$m_{1/2}$ plane for tanβ=50. The largest cross section at $m_0, m_{1/2} < 200$ GeV corresponds to low masses of squarks and gluinos. The event topology and kinematics of produced objects depend strongly on model parameters covering almost all possibilities expected in SUSY. In CMS the mSUGRA parameter plane is characterized by a set of benchmark points, shown in Table 1. Since the kinematics of muons is similar in all LM points, the LM0 ($m_0 = 200$, $m_{1/2} = 160$, $tan\beta$=10, A_0=-400, $sgn\mu = 1$) with the largest cross section has been chosen for reference. The large cross section offers the possibility to inspect this region of parameter space during the first year of LHC running at 10 TeV.

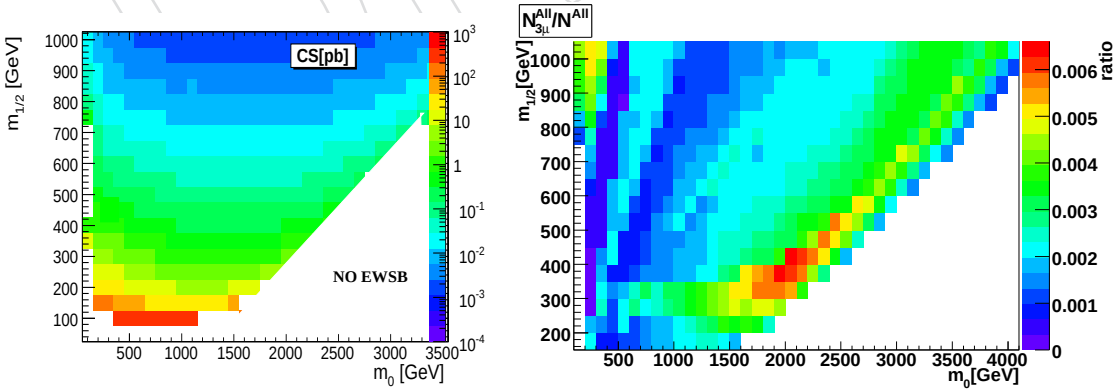

Figure 2: mSUGRA inclusive cross sections at 10 TeV and fraction of exclusive trimuon final state at $tan\beta = 50$.

The summary of SM background channels studied in this paper is presented in Table 1. The SM background channels can be split in groups according to the number of prompt isolated muons mostly appearing from Z or W leptonic decays and fake muons from jets:

1) The dibosons Z/γ^*W and ZZ productions (VV+jets) give at least 3 prompt muons and is the major irreducible background. Most of it can be suppressed by a veto on the Z invariant mass in the $M_{\mu\mu}$ distributions. However the γ^* contribution and wrongly reconstructed muons contribute to the signal region at $M_{\mu\mu} < 70$ GeV. Other channels, like WWW+jets and $t\bar{t}W$, have a negligible cross section ($< 0.5fb$) at LHC energies [8].

2) The $Z/\gamma^* \rightarrow \mu\mu + X$)+jets and $t\bar{t} \rightarrow W \rightarrow {}^{\circ -}) + X$ backgrounds with two prompt and one fake muon have much larger cross sections in comparison with diboson production and form a dangerous background for the trimuon final state. The WW+jets has a smaller cross section and is far less important. The gauge boson production is relatively well simulated at LHC energies, but the rate of fake muons from jets depends on numerous factors including uncertainties in soft gluon radiation and gluon splitting, jets fragmentation and reconstruction, muons isolation efficiency. These factors introduce large systematics in the estimation of these SM backgrounds.

3) The W+jets channel would require two fake muons and is expected to have small contribution in spite of large cross section. The QCD background with no prompt muons in the final state can be effectively suppressed by the trimuon requirement in spite of the large QCD cross sections.

Table 1: Signal and SM backgrounds data samples and cross sections used in this analysis.

MC sample	Generator	cs[pb] LO	Produced event
SUSY (m_0, $m_{1/2}$,tanβ, A_0, sqnμ)			
LM0 (200,160,10,-400,1)	SoftSusy+SusyHit+PYTHIA	110	200k
LM1 (60,250,15,0,1)	SoftSusy+SusyHit+PYTHIA	16.06	240k
LM2 (185,350,35,0,1)	SoftSusy+SusyHit+PYTHIA	2.42	240k
LM3 (330,240,20,0,1)	SoftSusy+SusyHit+PYTHIA	11.79	240k
LM4 (210,285,10,0,1)	SoftSusy+SusyHit+PYTHIA	6.7	200k
LM5 (230,360,10,0,1)	SoftSusy+SusyHit+PYTHIA	1.94	230k
LM6 (85,400,10,0,1)	SoftSusy+SusyHit+PYTHIA	1.28	220k
LM7(3000,230,10,0,1)	SoftSusy+SusyHit+PYTHIA	2.9	240k
LM8 (1450,175,50,0,1)	SoftSusy+SusyHit+PYTHIA	2.86	200k
LM9(1450,175,50,0,1)	SoftSusy+SusyHit+PYTHIA	11.58	200k
LM10(3000,500,10,0,1)	SoftSusy+SusyHit+PYTHIA	6.55	200k
LM11(250,325,35,0,1)	SoftSusy+SusyHit+PYTHIA	3.24	210k
Standard Model			
VV+jets(V=Z,W $\rightarrow$ e,μ,τ)	MadGraph+PYTHIA	11.8	200k
Z+jets (W $\rightarrow$ e,μ,τ)	MadGraph+PYTHIA	3700	1M
fl*+jets	MadGraph+PYTHIA	580	100k
$t\bar{t}$	MadGraph+PYTHIA	317	1M
W+jets (W $\rightarrow$ e,μ,τ)	MadGraph+PYTHIA	40000	10M
QCD100to250 (HT=100-250GeV)	MadGraph+PYTHIA	$1.5\ 10^7$	15M
QCD250to500	MadGraph+PYTHIA	$4\ 10^6$	5M
QCD500to1000	MadGraph+PYTHIA	14000	5M
QCD1000toInf	MadGraph+PYTHIA	370	1M

3 Data samples and the analysis framework

The SUSY signal was calculated in a few steps. With the given mSUGRA parameters((m_0, $m_{1/2}$, tanβ, A_0, sgnμ) the sparticles mass spectrum has been calculated at the EW scale using the renormalization group equation implemented in SoftSusy v. 2.18 [3] package. The radiative corrections to decays of sparticles have been calculated with the SusyHit v1.3 [4] code. The Monte Carlo (MC) events have been simulated with PYTHIA [6] 6.25 using CTEQ5l PDF. All SM backgrounds have been simulated at tree level with the MadGraph [7] package interfaced to PYTHIA. The initial and final state radiation was calculated in PYTHIA for all produced samples. The pileup effects was considered negligible at 10 TeV and L$\sim 10^{30}$ and were not simulated. The summary of the signal and SM background channels studied in this paper is presented in Table 1. The LO cross sections for signal and backgrounds have been used in this analysis in estimation of statistics. The official CMS data samples available in the CMS database, simulated in summer 2008 and fall 2008 with the CMSSW 2.2 have been used. The full simulation has used the complete CMS detector in the 'ideal' configuration, the effects of miscalibration, misalignment were not considered in this study. All mSUGRA benchmark points have been simulated with the full simulations but for the discovery reach the signal was simulated in mSUGRA mass plane at tanβ=10, 50 ($A_o = 0$, sgnμ=1) using fast simulation (FASTSIM) of the CMS detector. The FASTSIM also has been used to produce some data samples for the study of MC generators.

The event reconstruction has been done with the CMS software version CMSSW 2.2.4 using CMS Physics Analysis Tools (PAT). The reconstructed and PAT objects have been extracted from data samples in grid jobs, stored in the private ntuple and analyzed in the local computer farm.

4 Event selection

This study has attempted to select SUSY using only muons, all other observables, including MET, jets have been avoided in order to reduce the systematic uncertainties and model dependencies of the search. The muons are considered as the most robust physics object in CMS. The selection of three prompt isolated muons is the main part of the analysis.

4.1 Muons selection

The selection of muons in trimuon search should give high suppression of fake muons from jets, provide large selection efficiency for different SUSY models and have a small sensitivity to systematic uncertainties. The muon identification was thoroughly studied at CMS [9] and 'standard' muon selection tuned to muons from Z/W decays include the following requirements:

- global muon consisting from the reconstructed track in the Tracker and Muon system with the global fit using all hits.
- muons track quality requirements such as number of hits in the Tracker $N_{hits} > 11$, and global track $\chi^2 < 10$.
- the relative isolation, which requires a low energy deposition in the cone around the muon track defined by $0.01 < \Delta R = \sqrt{\Delta\eta^2 + \Delta\phi^2} < 0.3$. An energy deposition $isoCal/PT_\mu + isoPT/PT_\mu < 0.1$ was required, where the calorimetric energy $isoCal$ and sum of the transverse momentum (PT) of all tracks $isoPT$ were weighted with the transverse momentum of the muon, i.e. low PT muons were required to be better

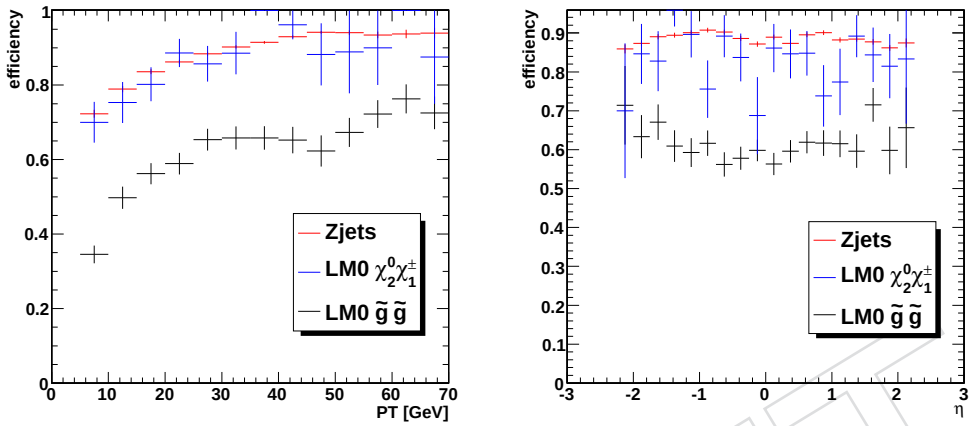

Figure 3: The PT and η dependence of the selection efficiency for the SM background and SUSY (LM0) muons from gaugino and gluino production.

isolated than high PT muons.

- vertex impact parameter calculated relatively to the beam position $d_0 < 0.02$ cm.

This selection gives a robust muon identification, especially at large transverse momentum PT typical for on shell decays of gauge bosons. The selection efficiency of the muons from SM background and SUSY (LM0) with the muon quality requirements and the 'standard' isolation is shown in Figure 3. There is a difference between SUSY muons and muons from bosons decays. The muons from low mass SUSY region are softer and more central as compare with the Z and W leptonic decays, see Figure 4. The SUSY events with gluino or squark production also have larger jets multiplicity in the central region which affects efficiency due to worser isolation, see Figure 3. This drop in efficiency results in factor ~ 2 smaller trimuon selection efficiency for the gluino-squark decays in comparison to the direct neutralino-chargino production.

Fake muons in the SUSY search are all muons, which are not coming from hard interactions, decay of gauge bosons or SUSY decays. These are categorized as follows:

1. Muons from decays of heavy flavor quarks (b,c) produced in a hard interaction or in soft gluon splitting. After isolation this is the main source of fake muons. Such fakes can be identified by a displaced vertex.

2. The muons from decays of long living mesons (K, π). Such muons can be suppressed by tighter isolation cuts.

3. The calorimeter punch through can produce some tracks in the muon system. Such fakes can be suppressed by the hit pattern in muon chambers and give negligible contribution for the considered detector model.

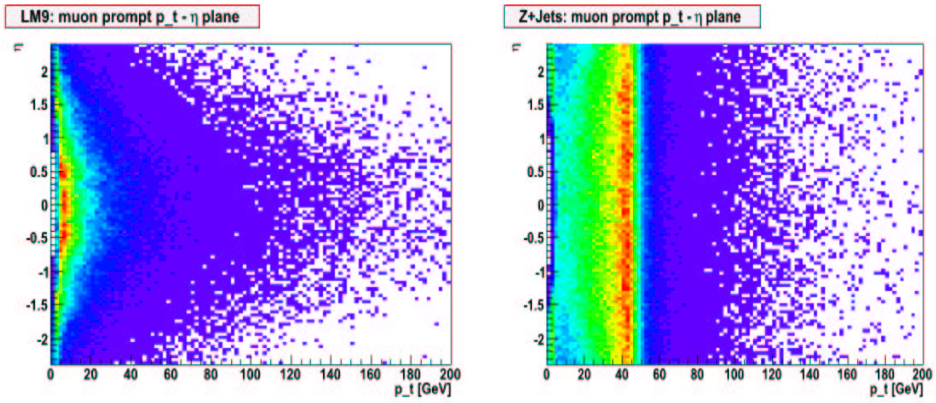

Figure 4: The PT distribution of fake muons after loose isolation cuts ($isoPT < 5$ GeV/c) for different MC generators(left) and different production channels (right). The distributions are normalized to the number of events.

The contribution of fake muons from heavy flavor decays has large uncertainties. The production of hard heavy flavor jets can be calculated at matrix element level, but the contribution of heavy flavors from soft jets produced in the parton shower evolution is far less known, since it is sensitive to the gluon splitting probability into heavy quarks. The sensitivity to MC details is demonstrated in Figure 5, which shows the PT distributions of fake muons in the Z=jets sample after loose isolation $isoPT < 5$ GeV/c cut for ALPGEN and SHERPA. The fake rate differs by up to 60% depending on the muon PT.

Contrary the fakes from jets produced in different channels with the same generator are rather similar and the fake rate mostly depends on the heavy flavor content of the event. SUSY and $t\bar{t}$ have practically the same fake rate per event, while the fake rate for QCD (Njets) and electroweak boson production is an order of magnitude lower.

The muons produced in a jet can be isolated when the corresponding jet is too soft or the muon angle with respect to the jet axis $sin\theta_\mu = \frac{m_B - m_D}{2p_\mu m_D}$ is too large. Thus the suppression of fakes requires a careful tuning of isolation and impact parameters. These parameters have their own instrumental uncertainties related to the calorimeter energy scale, track momentum resolution, efficiency and impact parameter uncertainties. These uncertainties may not be fully covered by the simulation model. Minimization of the fake rate and reduction of systematics can be better done from experimental data by optimizing the cuts using a pure sample of 'prompt' and 'fake' muons. The selection of these samples will be described in the next section. Then the cuts from this data driven optimization will be compared with optimized cuts using as prompt sample SUSY MCs, the so-called MC truth samples. It will be shown that they are in the same range of efficiency and rejection, thus paving the way for using reference data samples for the muon selection. This has the big advantage that one can optimize the muon cuts for a minimum fake rate using realistic vertex and isolation distributions.

4.1.1 Selection of reference samples

Two samples have been used: the QCD dijets enriched with 'fake' muons and the Z($\mu\mu$) with 'prompt' muons. The selection of samples has been optimized to get the highest purity of the samples. The samples have been preselected with the high level trigger (HLT) streams: DiJet70 ($ET_j > 70$ GeV) for QCD and the double muons DoubleMu3 ($PT_\mu > 3$ GeV/c) for the Z($\mu\mu$). Then an exhaustive list of observables have been considered to minimize the fake rate by comparing these samples. This was done with a Genetic Algorithm (GA) [10], which

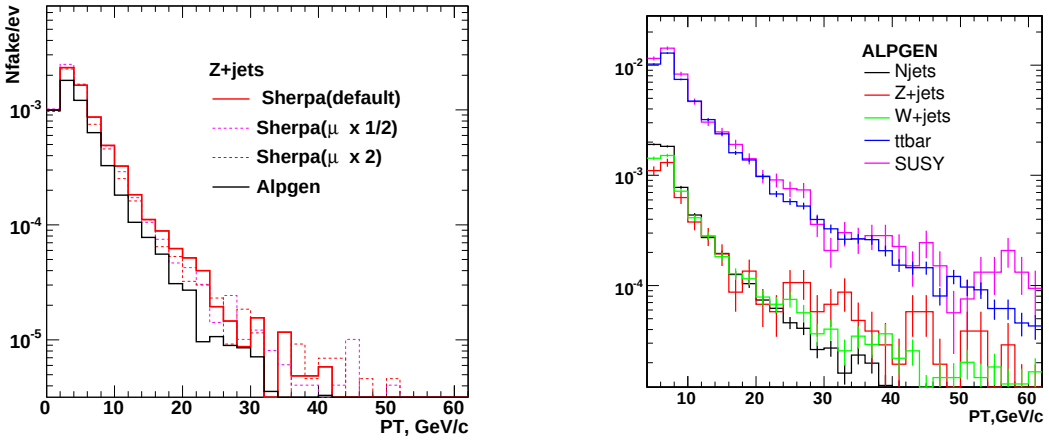

Figure 5: The PT distribution of fake muons after loose isolation ($isoPT < 5$ GeV/c) for different MC generators(left) and different production channels (right).

selected the most sensitive parameters from the following list: MET, sum of ET, jets, muon kinematics, angular relations, invariant mass of dijets and dimuons, jet balance parameters, etc. After ranking of all input variables by the GA, the following observables have been used for the final selection: the number of jets N_j with $ET_j > 30$ GeV and $|\eta| < 2.4$, the number of reconstructed muons N_μ with $PT_\mu > 5$ GeV/c and $|\eta| < 2.1$, the missing energy calculated as a recoil of all selected jets and muons in the event MET_{rec}, the transverse energy of all selected jets and muons $ET_{eff} = \Sigma ET_j + \Sigma PT_\mu$, the azimuthal angles between leading jets $\phi(j1, j2)$, jets balance parameters $\alpha 2 = ET_{j2}/Minv(j1, j2)$ and the transverse invariant mass of the MET_{rec} and the leading muon $M(MET, \mu)$.

The selection cuts optimized with GA using the statistics corresponding to L_{acc}=100 pb^{-1} are presented for both reference samples in Tables 2 and 3. Around 10^7 fake muons can be selected with a contamination of $\sim 10^{-4}$, which originate mostly from W+jets. The Z-sample delivers a high purity sample of $\sim 10^4$ prompt muons. The robustness of the selections has been checked by changing the jet energy scale by $\pm$10%. This affects the contamination by $\sim$ 20% for the fake sample and $\sim$ 40% for the prompt sample, which is acceptable given the small contaminations.

4.1.2 Optimization of the muon selection

The two reference samples for fake and prompt muons discussed above can be used to optimally separate fake muons from prompt muons using a GA with the three major parameters: relative isolations $isoPT/PT_\mu$, $isoCal/PT_\mu$ and impact parameter dxy calculated relatively to the vertex with the highest sum of PT of all tracks coming from this vertex. Usually this is the main vertex of the event. All muons have been subjected to the quality cuts $N_{hits} > 11$ and $\chi^2 < 10$. The resulting parameter cuts after the optimization are presented in Table 4. The stability of the selection is illustrated in Figure 6, which shows the efficiency of prompt and fake

Table 2: Selection criteria of the fake reference sample (left) and expected statistics of fake muons from QCD at L_{acc}=100 pb^{-1}.

Observables	selection
HLT Trigger	DiJet70
N_j	=2
$\phi(j1, j2)$	160^o-180^o
$\alpha 2$	<0.42
N_μ	>0
$M(MET, \mu)$	<40GeV
MET_{rec}	<100GeV

Sample	HLT[%]	Nev 100 pb^{-1}
QCD100to250	78	9430000
QCD250to500	100	362000
QCD500to1000	100	15900
QCD1000toInf	100	386
$t\bar{t}$	99	112
W+jets	25	905
Z+jets	38	338
VV+jets	60	1.4

Table 3: Selection criteria of the prompt reference sample and number of expected prompt muons ($\times 2$) from Z+jets and VV+jets at L_{acc}=100 pb^{-1}.

Observables	selection
HLT Trigger	DoubleMu3
N_μ	=2
$M_{\mu^+\mu^-}$	70-180 GeV
N_j	<2
MET_{rec}	<100GeV
ET_{eff}	<120GeV

Sample	HLT[%]	Nev 100 pb^{-1}
Z+jets	35	42560
VV+jets	52	140
QCD100to250	5	0
QCD250to500	10	0
QCD500to1000	17	0
QCD1000toInf	29	0
$t\bar{t}$	48	1
W+jets	26	2.7

muons as function of each of the three major parameters. The 'signal-over-noise' ratio, defined as $N_{prompt}/\sqrt{N_{prompt} + N_{fake}}$, is shown by the dashed-dot line on the scales on the right-hand side. The sensitivity to $\pm 5\%$ variations at each value of the parameter is shown by the dashed line and can be read off at the vertical scale on the right-hand side. In this stability plot one parameter has been changed at once. The optimized selection cuts are in a stable region and correspond to a high efficiency for prompt muons.

The minimization of the fake rate was repeated using the prompt muons from the SUSY(LM0) sample and fake muons from all considered SM backgrounds. Here the prompt muons were excluded from the SM background samples, so these samples are referred to as MCtruth samples. The distribution of the muon selection parameters for the MCtruth samples is shown in Figure 8. The results of the optimization for prompt muons from Z+jets is similar to the optimization for the MC truth samples, as can be seen from Table 4. The stability and efficiencies plot, similar to the Figure 6 is shown in Figure 7.

In principle one could reweight the prompt muons from Z-decay with respect to the SUSY muons in the $PT - \eta$ plane. The result of the optimization of such reweighted Z-muons is also shown in Table 4.

All selection cuts are rather similar and are in the stable efficiency region. Throughout the rest of the analysis the 'tight' muon selection, close to the obtained from the reference samples has been used: $isoCal/PT < 0.08$, $isoPT/PT < 0.08$, $dxy < 0.004$ cm and quality requirements (global track $\chi^2 < 10$, track $N_{hits} > 11$), since this selection can be obtained directly from the data using the reference samples. The selection efficiency of the SUSY muons with this cuts is shown in Figure 10 and is similar to the efficiency using the 'standard' muon cuts, shown before in Figure 3.

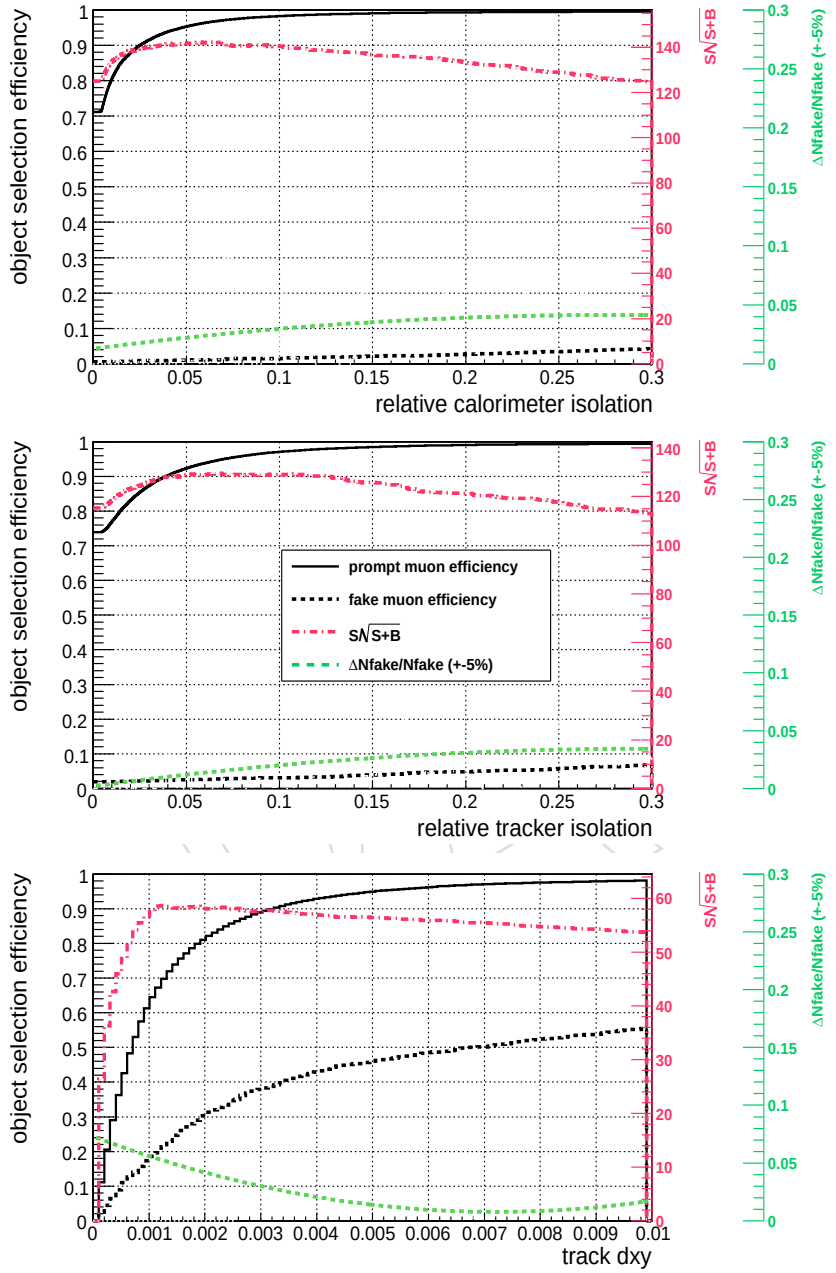

Figure 6: The efficiency of the prompt and fake muon selection together with the signal significance and sensitivity as function of the three muon selection variables (from top to bottom) after minimizing the fake rate using the QCD and Z reference samples for fake and prompt muons, respectively.

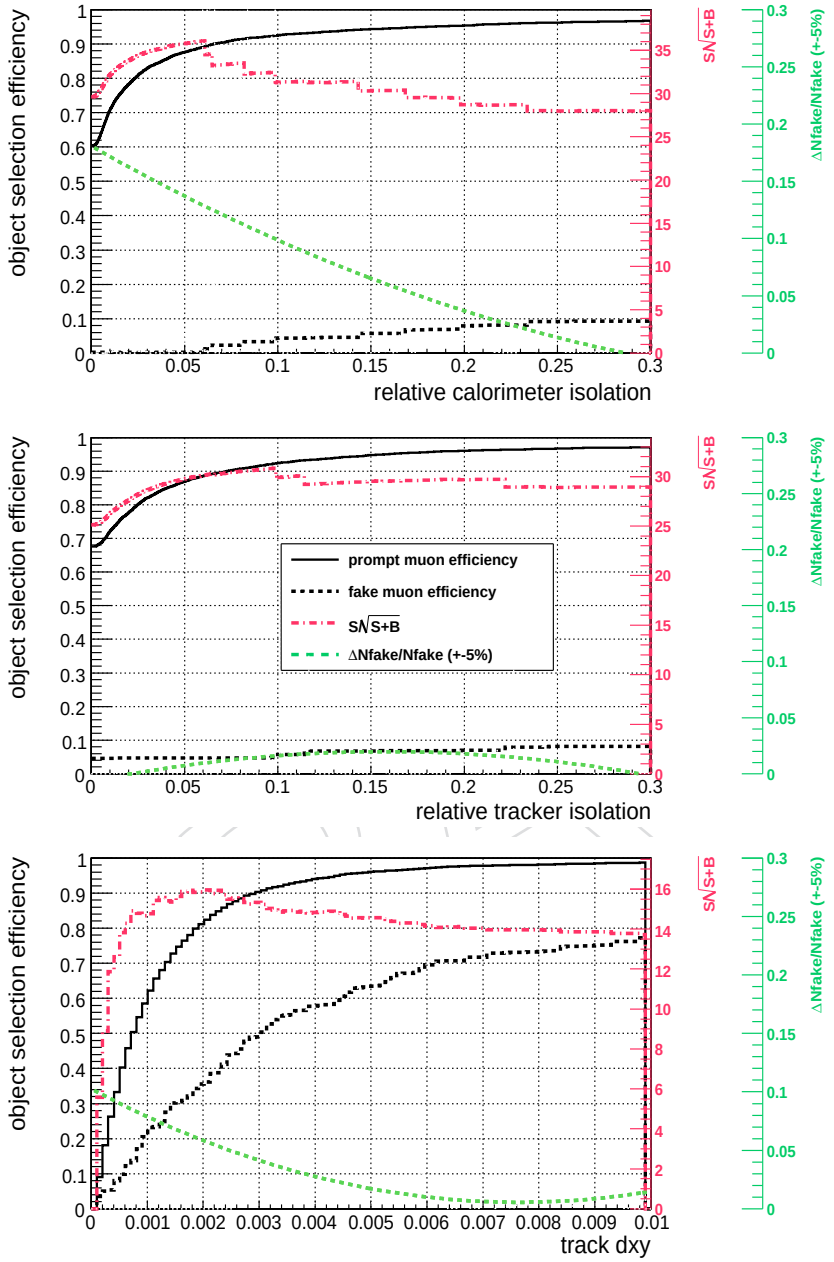

Figure 7: The efficiency of the prompt and fake muon selection together with the signal significance and sensitivity as function of the three muon selection variables (from top to bottom) after minimizing the fake rate using the SM backgrounds and SUSY(LMO) samples for fake and prompt muons, respectively.

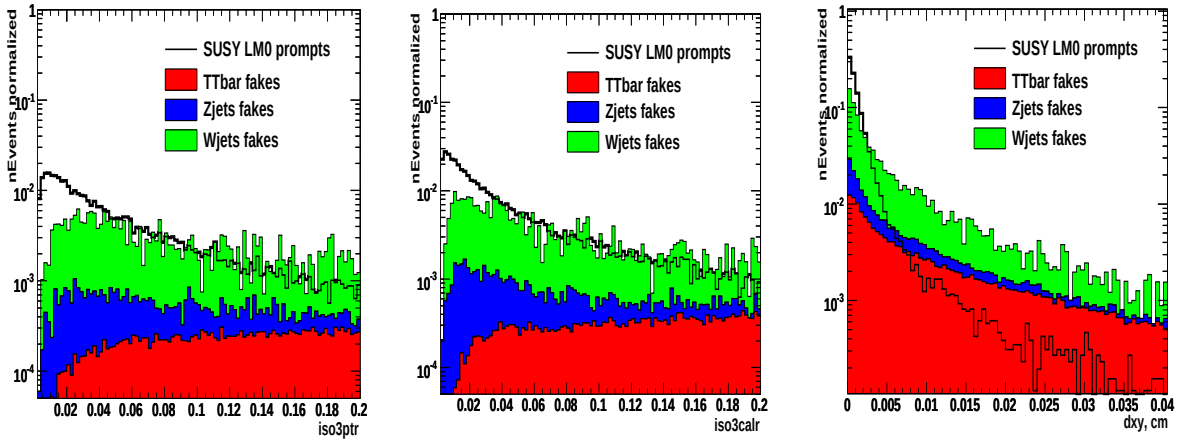

Figure 8: Relative isolations $isoPT/PT_{\mu}$, $isoCal/PT_{\mu}$ and impact parameter dxy in MCtruth samples of SUSY (LM0) and SM backgrounds.

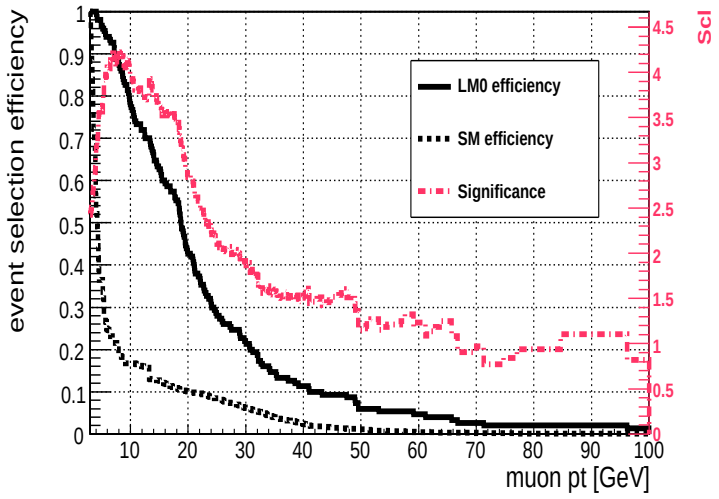

Figure 9: The optimization of the PT selection of SUSY muons.

The same selection was applied to all three muons. Indeed the relative isolation will automatically increase the efficiency for the hardest muons in the event, while still keeping high suppression of fake muons, which are soft. The looser cut on the impact parameter for harder muons does not improve efficiency significantly.

The cut on the muon transverse momenta is an another sensitive measure to reduce background. Since the SUSY muons are all soft for the parameter range of low SUSY masses, which we consider, the minimum PT cut was selected to be the same for all three muons. This cut was optimized by scanning the significance and signal efficiency for the SUSY and SM backgrounds after the trimuon selection. The fake and SUSY muon efficiencies are shown in Figure 9 as function of the muon PT cut together with the significance of the signal. The selected threshold ($PT > 8$ GeV/c, $|\eta|$ <2.1) corresponds to the onset of the fakes contribution, which rises fast at low PT. The selection efficiency of the isolation and impact parameters is presented in Table 5. The relative isolation cut strongly suppress $t\bar{t}$ and and $Z/\gamma*$+jets.

Table 4: Selection of muons

parameter	reference samples (QCDfake-Zprompt)	reference samples weighted	MCtruth (SUSY-SMbkg)
$isoCal/PT$	< 0.075	< 0.081	< 0.09
$isoPT/PT$	< 0.084	< 0.091	< 0.15
dxy,cm	< 0.0035	< 0.0035	< 0.0026

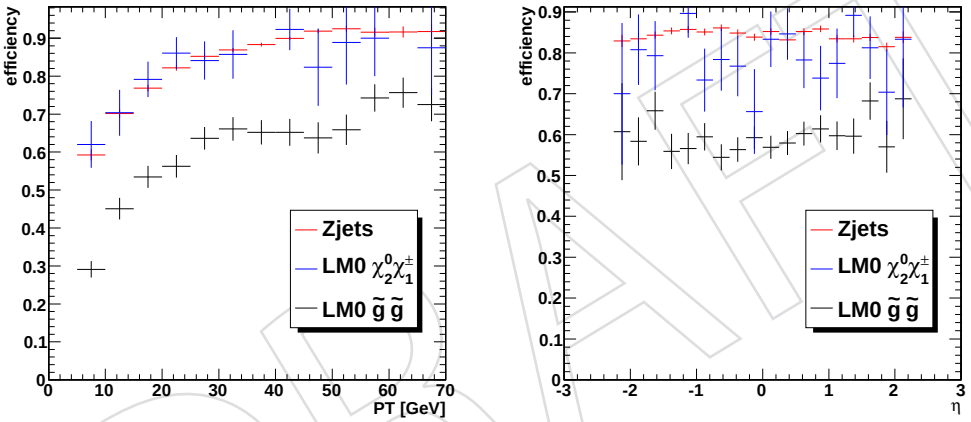

Figure 10: Selection efficiency of SUSY muons and SM backgrounds with the optimized cuts used in the study.

Table 5: Trimuon selection efficiencies (to the previous steps) for the 'tight' muons selection.

	quality cuts ($\chi^2 < 10$, $N_h > 11$)	Impact parameter $dxy < 0.004$ cm	Relative isolation < 0.08
LM0	0.91	0.32	0.26
LM1	0.92	0.50	0.38
VVJets	0.91	0.87	0.75
Z+Jets	0.84	0.43	0.01
γ*+jets	0.84	0.48	0.07
$t\bar{t}$	0.90	0.16	0.004
W+jets	0.86	0.74	0

4.2 SUSY trimuon selection

After the muon identification was optimized, the event selection is simple in the trimuon analysis. Exactly three muons have been selected with an opposite sign pair. The statistics for the signal and all SM backgrounds with different selections is presented in Table 6 for L_{acc}=400 pb^{-1}. The third column shows the number of muons at generator level. For the signal (LM points) this is the number of event with exactly three MC prompt muons. For backgrounds the number in the Table 6 corresponds to events with at least three MC muons, independent prompt or fake. The selection of two 'tight' muons with one or more extra reconstructed ('reco') muon (PT >8 GeV/c, $|\eta| < 2.1$) in the fourth column demonstrates the efficiency of the third muon selection. Since more than three muons are allowed, the number of event can exceed the number obtained at MC level. With only two 'tight' muons main background is coming from Z+jets and $t\bar{t}$ with one fake muon. The Z-containing background can be effectively suppressed with the selection on invariant mass of OS muons $M_{\mu^+\mu^-} \neq M_Z$. Two combinations of OS pairs can be built, with low PT OS pairs and with high PT pairs. One OS combination has wrong pairing but the muons from neutralino and chargino have similar kinematics and using all OS combinations would slightly increase the signal significance. The low PT combination is also beneficial because moves all signal event to lower invariant masses away from the Z peak. The invariant mass of OS muons for the selection two 'tight' plus at least one 'reco' muon is presented in Figure 11 for low PT and all OS pairs. The low PT pairing of OS muons reduces the Z peak in the Z+jets events due to wrong combination of the muon from Z and the fake muon. The LM0 signal is visible but the shape of the background is very similar and the magnitude depends on the fake rate. While the Z+jets background can be controlled by the Z peak, the contribution of the $t\bar{t}$ is hard to estimate. Moreover almost half of signal events (LM0) are selected with the fake muon. This drives analysis to the more tight cuts on the third muon. The final selection of three 'tight' muons results in $N_{LM0} = 26.3 \pm 2.4(stat)$ events expected from SUSY (LM0) with the SM background of $N_{bkg} = 12.13 \pm 2.44(stat)$ at L_{acc}=400 pb^{-1}. The statistical errors correspond to the size of available MC samples. The event selection using the 'standard' cuts gives $N_{LM0} = 29.1 \pm 2.5$ signal and $N_{bkg} = 23.5 \pm 4.1$ of background.

With such 'tight' selection the biggest contribution is coming from irreducible ZW background, the $Z/\gamma*$+jets and $t\bar{t}$ are following. The invariant mass distribution of all OS pair and the lowest PT pair after trimuon selection is presented in Figure 12. The contribution of Z containing backgrounds and contribution from heavy resonances Υ, J/Ψ at low $M_{\mu\mu}$ can be suppressed by requing invariant mass of all OS in the range of $M_{\mu\mu}$[10,75] GeV. All OS combinations contain the correct pairing of muons together with the combinatorial background. With enough statistics (L_{acc} >1 fb^{-1}) this combinatorial background can be subtracted revealing the kinematic end point of the $M_{\mu\mu}$ distribution in SUSY neutralinos decay. The statistics for the low and all OS pair combinations in the $M_{\mu\mu}$[10,75] range is shown in the Table 6 in the last columns.

4.3 Trigger

The most suitable trigger streams for the trimuon signature are either the single muon Mu9 ($PT_\mu > 9$ GeV/c) or the double muons DMu3 ($PT_\mu > 3$ GeV/c). The selection efficiency for the SUSY LM points and SM backgrounds before and after offline selection is shown in Table 7 for these two trigger streams. The dimuons trigger is efficient for all SUSY LM points and in addition has an advantage of having ~ 5 times smaller size of the corresponding data sets.

Table 6: Statistics for final selection of trimuon state at 400 pb^{-1}. The errors corresponds to the size of MC samples.

	cs[pb]	N_μ^{MC}=3	N_μ=2'tight' +≥1 'reco'	N_μ=3 'tight'	low PT OS pairs M[10,75]GeV	all OS pairs M[10,75]GeV
SUSY						
LM0	110	101	186.3 ± 6.4	26.30 ± 2.4	23.7 ± 2.27	35.38 ± 2.77
LM1	16.06	29.6	31.0 ± 1.4	6.90 ± 0.65	6.00 ± 0.61	9.81 ± 0.78
LM2	2.42	3.9	1.8 ± 9.1	0.30 ± 0.04	0.18 ± 0.04	0.23 ± 0.04
LM3	11.79	14.84	22.9 ± 1.0	3.50 ± 0.40	2.09 ± 0.30	2.67 ± 0.33
LM4	6.7	6.6	10.5 ± 0.6	2.40 ± 0.30	0.97 ± 0.18	1.07 ± 0.19
LM5	1.94	0.98	1.9 ± 0.1	0.30 ± 0.04	0.16 ± 0.03	0.20 ± 0.03
LM6	1.28	3.58	4.1 ± 0.1	1.10 ± 0.06	0.86 ± 0.06	1.22 ± 0.07
LM7	2.9	3.56	4.1 ± 0.3	0.84 ± 0.12	0.61 ± 0.11	0.82 ± 0.12
LM8	2.86	7.508	1.6 ± 0.1	0.27 ± 0.04	0.14 ± 0.03	0.15 ± 0.03
LM9	11.58	13.8	17.5 ± 0.6	3.40 ± 0.30	3.2 ± 0.26	5.1 ± 0.33
LM10	6.55	0.12	0.17 ± 0.01	0.04 ± 0.003	0.017 ± 0.002	0.02 ± 0.002
LM11	3.24	8.02	8.5 ± 0.3	1.40 ± 0.13	0.70 ± 0.09	0.90 ± 0.11
SM						
VVJets	11.8	36.2	18.5 ± 0.9	8.80 ± 0.70	4.35 ± 0.46	5.60 ± 0.52
Z+Jets	3700	21195	973 ± 33.8	1.20 ± 1.10	1.17 ± 1.17	1.17 ± 1.17
γ^*+jets	580	993	150 ± 17.4	2.02 ± 2.02	2.02 ± 2.02	4.05 ± 2.86
$t\bar{t}$	317	1737	204± 5.2	0.13 ± 0.13	0	0
W+Jets	40000	225.5	0	0	0	0
QCD	0.15mb	2368726	0	0	0	0
ΣSM	-	2392913	1346± 38	12.13 ± 2.44	7.55 ± 2.53	10.83 ± 3.26

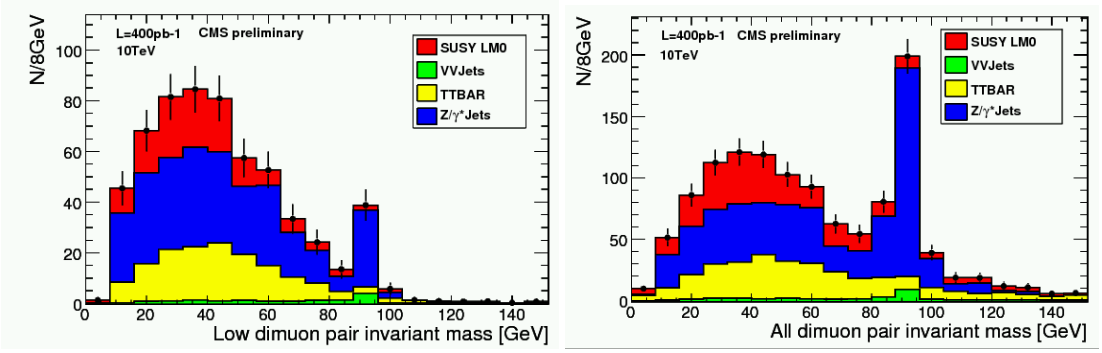

Figure 11: Invariant mass distribution of the lowest PT OS muons combination and all OS combinations after 2 'tight' and at leat one 'reco' muons selection in SUSY (LM0) and SM backgrounds at 400 pb^{-1} and 10 TeV.

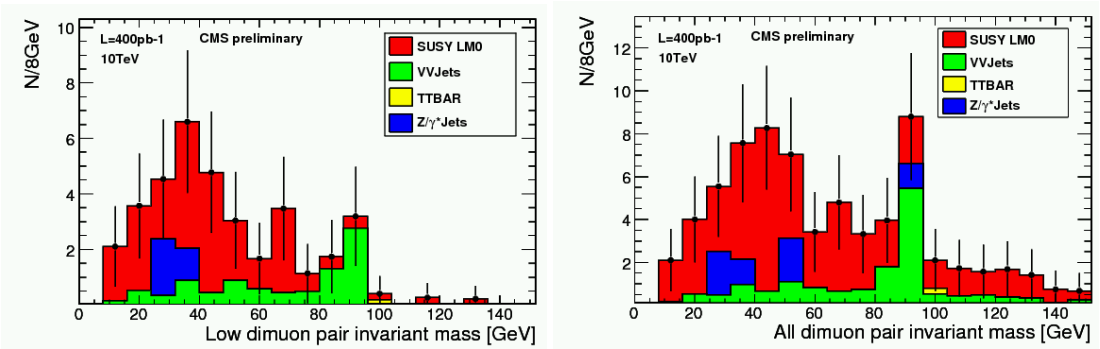

Figure 12: Invariant mass distribution of the lowest PT OS muons combination and all OS combinations after 3 'tight' muons selection in SUSY (LM0) and SM backgrounds at 400 pb^{-1} and 10 TeV.

Table 7: Trigger efficiency [%] of single muons (Mu9) and double muon (Dmu3) trigger streams before and after offline trimuon selection.

channel	inclusive Mu9	inclusive DMu3	trimuon Mu9	trimuon DMu3
SUSY				
LM0	28.6	10.22	100	100
LM1	22.7	8.15	99.6	100
LM2	21.3	7.43	99.2	100
LM3	28.4	11.25	100	100
LM4	21.8	7.44	100	100
LM5	23.5	8.16	100	100
LM6	30.3	10.6	99.8	100
LM7	21.8	6.57	100	100
LM8	37.7	17.7	100	100
LM9	24.5	9.86	100	100
LM10	25.9	7.42	100	100
LM11	27.1	9.39	100	100
SM backgrounds				
VV+jets(V=Z,W)	42.1	10.1		
Z+jets	27.4	14.7		
γ^*+jets	12.2	9.18		
$t\bar{t}$	28.9	8.45		
W+jets	18.4	0.089		
QCD100to250	0.68	0.075		
QCD250to500	2.04	0.28		
QCD500to1000	4.17	0.74		
QCD1000toInf	7.31	1.88		

Table 8: Summary of systematic uncertainties

Observable	Source	Range	$\Delta N/N$
Tracker isolation	Tracker resolution	$\pm$ 2%	$\sim$0%
Calo isolation	Energy scale	$\pm$10%	1.6%
Muon PT	Tracker resolution	σ_{pt}	$\sim$0%
Track impact dxy	Tracker resolution	σ_{dxy}	7.6%
SM cross section	theory		5 %
PDF	theory		2%
luminosity	detector		5%
Total syst. uncertainties			10.7%

5 Systematic uncertainties

The summary of the anticipated instrumental uncertainties affecting the muon selection is presented in Table 8 and includes: energy scale, momentum and impact parameter resolutions. The parameters have been changed in the indicated ranges and the variations in the number of selected events $\Delta N/N$ was counted. These instrumental uncertainties amount to $\sim$ 7.9%, if added in quadrature.

Theoretical uncertainties include uncertainties in the parton distribution functions (PDF) and uncertainties in the SM background cross section. The PDF uncertainties have been studied with the re-weighting technique using the LHPDF libraries [2] and contribute $\sim$ 2%. The errors in the SM cross sections at 10 TeV have been estimated by comparing SM cross section calculated with ALPGEN, SHERPA and MCNLO generators. For the Z+jets, W+jets, ZW and $t\bar{t}$ the uncertainties in cross section are estimated to be below 5%. The uncertainties in the luminosity estimation adds up another 5% yielding in total $\sim$ 10.7%, if added in quadrature, i.e. assuming no correlations between different sources. The considered uncertainties do not change the results significantly, especially since the SM backgrounds are experimentally determined from the side bands using the ABCD method. In this case the theoretical uncertainties are given by the data themselves and also a large fraction of the experimental uncertainties, like vertex uncertainties, is propagated from the side bands to the signal region.

6 Data driven background estimation

The main SM background in the trimuon selection is coming from ZW with three prompt muons and Z/$\gamma*$+jets, $t\bar{t}$ with one fake muon. The data driven optimization of muon selection and the use of the reference samples for model validation would reduce systematic uncertainties in the SUSY search. The residual uncertainties can be further reduced or eliminated by using the data driven background estimation. The data driven methods extrapolate the SM background contribution from control regions, where uncertainties are controlled, to the signal region. Below two methods are used to estimate contributions from fake and Z-containing backgrounds.

6.1 Contribution of fake muons

The contribution of fake muons into the signal sample has been studied with the ABCD method applied to the weakly correlated isolation ($isoPT/PT$,$isoCal/PT$) and impact parameter (dxy) of the muons. Here the assumption is made that the probability of two fakes in the selected event is small. The appearance of two fakes from jets is possible when the fakes suppression

is low, and can be spotted by large contribution of Z+jets in the invariant mass of OS muons M[75,100] GeV. The rate of same sign (SS) trimuons will also help to identify such case.

The events, after the selection of two OS tight muons with invariant mass M[10,75] GeV and at least one muon passing the quality and kinematic requirement (track N_{hits} >11, global track χ^2 <10, $PT > 8$ GeV/c, $|\eta| < 2.1$) are divided in four regions defined by the isolation and impact parameter of the third muon, see Figure 13. Region A, the signal region, contains events with 3 tight muons. In Region B the third muon is not isolated but passing the dxy selection, in region D the third muon is isolated but dxy rejected. Region C is populated with the major part of the fake backgrounds, here the third muon is not isolated and also not passing the dxy requirement.

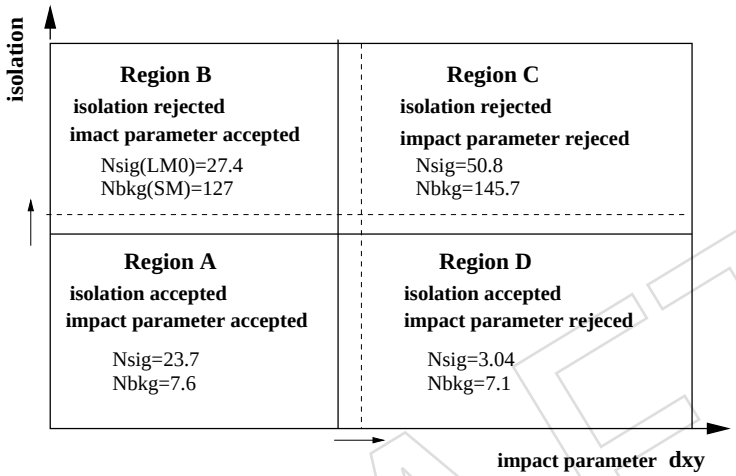

Figure 13: ABCD method for the estimation of the residual fake muons contribution.

In order to work the parameters should have no or only linear correlation in the considered range. Then the contribution from control regions B,C,D to the signal region A can be calculated from simple ratio A=B×D/C. Else the proportionality of the events in the different regions is not guaranteed. Furthermore the data should be factorisable in the selected parameters. The validity of these constraints can be verified by checking the following ratio r_{abcd}=A×C/B×D==1 in the considered ranges of parameters. The distribution of the significance of this ratio (1-r_{abcd})/σ_r is presented in Figure 15 for the selected SUSY (LM0) and SM background samples, here σ_r is the statistical error. The 2-dimensional distribution in Figure 15 was obtained by moving the isolation and impact parameter cuts away from the signal region A with small steps and calculating the significance of the ratio for each point. The size of the signal region A was kept constant. Such a distribution, obtained from 'real' data, proves the validity of the method. Any large local deviations or structures in the distribution will limit use of the method. The observed value of the double ratio consistent with one proves that the method works in the range of cuts considered.

Another way to verify the method, the so-called closure test, would consider differences between number of events estimated from the ABCD N_{abcd} and predicted from the MC truth N_{mc}. The significance parameter $|N_{abcd} - N_{mc}|/\sigma_n$ for signal region A was calculated and plotted in Figure 15. Again, no large deviations from one has been observed. Thus the isolation and impact parameter of fake candidate are only weakly correlated in the selected trimuon events. However the third muon used as a fake candidate in this method has also some contribution from prompt muons coming from ZW and SUSY signal. In addition there are fake muons which

are coming from SUSY. These contaminations affect the performance of the ABCD method. Figure **??** shows the similar plots without SUSY contributions.

Therefore the correlation of the parameters have been checked with the 'signal free' QCD reference sample. Figure 16 shows the significance of the ratio and the closure plot obtained for the fake muons from the QCD reference sample with one selected muon. The selection cuts have been moved through all the range of parameters and the significances have been calculated. Again, with much large statistics no correlations have been observed.

The results of the background estimate with and without signal contamination are presented in Table 9. The conservative estimate of 10.7% systematic uncertainties is taken into account. The numbers corresponds to the number of events selected in the invariant mass range M[10,75] GeV for low PT pairs and for number of all OS dimuon combinations. Using the 'tight' muon cuts and including only SM backgrounds with fake muon, the estimated background for the low PT pairs results in 5.1$\pm$0.52(sys) events in reasonable agreement with 3.2 expected events at 400 pb^{-1}. The addition of the ZW background with prompt muons increase the estimate to 6.20$\pm$0.66(sys). Including also the SUSY (LM0) signal results in 7.98$\pm$0.86(sys) events in the signal region, mostly coming from SUSY fake muons.

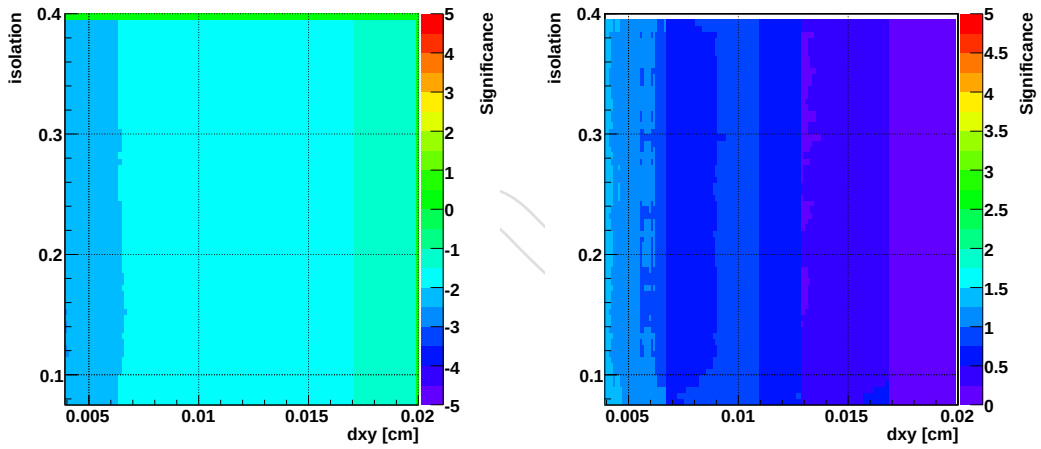

Figure 14: Left: the significance of (1-A·C/B·D)/σ) parameter in isolation-dxy plane obtained with selected sample of 2 'tight' muons and at least one reco muons. Right: the significance of predicted and estimated number of events in the signal region $|N_{abcd} - N_{mc}|/\sigma$.

6.2 Contribution of prompt muons.

The ZW channel has similar to SUSY final state topology and is the control measurement for the trimuon SUSY search. The observation of the Z peak (Z-candle) in the selected trimuon events can be used to calibrate the selection efficiency. On the other hand the ZW is also an important background, especially with the off-shell Z and γ* muonic decays. The contribution of the ZW background into the selected sample can be estimated from the events in the $M_{\mu\mu} = M_Z[85, 95]$ GeV invariant mass range, mostly populated by events with Z($\mu\mu$). The number of events in

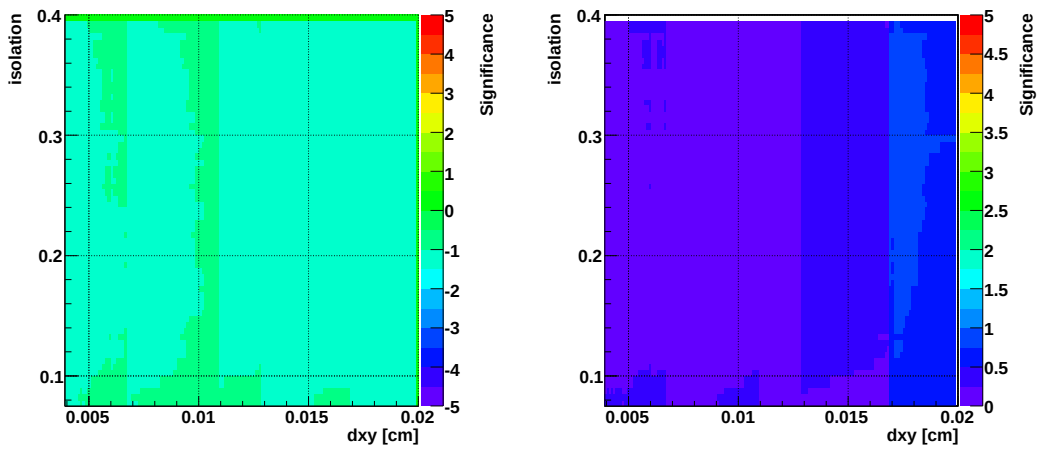

Figure 15: Left: the significance of (1-AC/BD)/σ) parameter in isolation-dxy plane without SUSY signal. Right: the significance of predicted and estimated number of events in the signal region $|N_{abcd} - N_{mc}|/\sigma$.

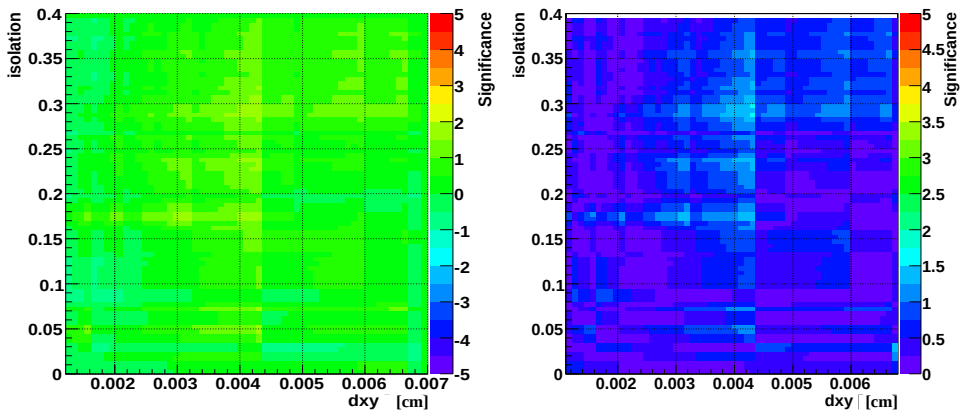

Figure 16: Left: the significance of (1-AC/BD)/σ) parameter obtained with the QCD reference sample. Right: the significance of predicted and estimated numbers in the signal region $|N_{abcd} - N_{mc}|/\sigma$ for the QCD sample.

the signal region M[10,75] GeV can be calculated from the $Nsig = N_{M[85,95]} \cdot R$, where the MC correction factor is $R = N^{MC}_{M[10,75]}/N^{MC}_{M[85,95]} = 0.877 \pm 0.058(stat) \pm 0.018(sys)$ for all OS pairs and $R = 1.572 \pm 0.133(stat) \pm 0.031(sys)$ for the low PT OS combinations. The factor has been calculated from the MC truth ZW sample. The systematical error corresponds to the theoretical uncertainties obtained by comparing predictions from ALPGEN, SHERPA and MCNLO. As for the ABCD method, such an estimation suffers from contaminations coming from SUSY and SM background with fake muons (Z+jets and $t\bar{t}$). The SUSY contamination his coming from on shell Z decays of neutralinos and the combinatorial background.

The Z candle method without SUSY contamination signal predicts 5.11± 0.56(sys) of low PT OS muons in the signal invariant mass range M[10,75] at 400 pb^{-1}. This is in good agreement with expectations from MC truth simulations, which yield 4.35. The contamination from SUSY (LM0) slightly increases the prediction to 5.78 ± 0.63(sys). The all OS pairs gives similar performance, see Table 8. The errors here include systematic uncertainties considered in the previous section.

The SM background estimation for from the data driven methods yields for low PT pairs 13.76 ± 1.06(sys) to be compared with 7.55 ± 0.81(sys) obtained from the event selection based on the MC truth information. The signal contamination overestimates the background obtained from data and gives more conservative limits in SUSY discovery.

Table 9: Summary of data driven (DD) estimation of SM backgrounds at 400 pb^{-1}

	low PT OS muons M[10,75]GeV	all OS muons M[10,75]GeV
Selection Cuts:		
NSignal(LM0)	23.7 ± 2.27(statmc) ± 2.53(sys)	35.38 ± 2.77(statmc) ± 3.78(sys)
NBkgMC	7.55 ± 2.53(statmc) ± 0.81(sys)	10.83 ± 3.26(statmc) ± 1.16(sys)
DD estimate:		
DD without SUSY:		
NBkg Z candle	5.11 ± 0.56	6.41 ± 0.7
NBkg ABCD	6.20 ± 0.66	6.30 ± 0.67
NBkgDD total	11.31 ± 0.86	12.71 ± 0.97
with SUSY signal(LM0):		
NBkg Z candle	5.78 ± 0.63	8.69 ± 0.95
NBkg ABCD	7.98 ± 0.86	9.42 ± 1.0
NBkgDD total	13.76 ± 1.06	18.11 ± 1.38

7 Discovery reach

The discovery reach for the trimuon SUSY final state was calculated with the mSUGRA FASTSIM scan in $m_0 - m_{1/2}$ plane for tanβ=10,50 and $A_0 = 0$, sgnμ=1. The statistical errors and systematical uncertainties have been treated with the RooStat package [11] using profile liklehood method. The significance and confidence interval have been calculated.

Using the data driven background estimation the LM0 SUSY model can be observed in low PT pairs with 5σ at L_{acc}=405 pb^{-1}. For the background estimates from the MC truth samples this limit decreases to L_{acc}=280 pb^{-1} Figure 17 shows discovery reaches calculated with the data driven estimation of the SM backgrounds using the low PT OS muons. The discovery reach at 400 pb^{-1} is limited to a narrow region at low masses and extends to the low $m_{1/2}$ with

increased accumulated luminosity. For even higher L_{acc} the selection efficiency of the SUSY trimuon analysis drops at $m_{1/2} \sim 250$ GeV, where the neutralino starts to decay via an on shell Z and the Z containing SM background can be suppressed only with extra selections on MET and jets.

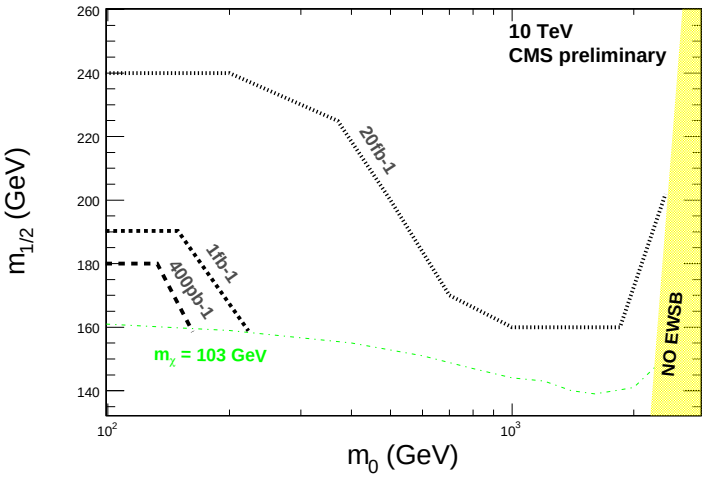

Figure 17: The SUSY trimuon(low PT OS) 5 σ discovery reaches and 95% exclusion limit obtained with the data driven background estimation at 10 TeV(mSUGRA tanβ=10, and $A_0 = 0$, sgnμ=1).

8 Conclusion

The selection of three isolated prompt muons without extra requirements on missing energies and jet multiplicities avoids the large instrumental and systemic uncertainties associated with these variables, which is important for SUSY searches using the first LHC data. The fact that the 3 leptons from the leptonic decays in the ZW production form an irreducible background in this data allows to prove the validity of the analysis, if the correct cross section for this channel is found.

The analysis has followed the data driven strategy in the selection of muons and estimation of SM background contributions. The optimization of the muon selection with reference QCD and Z samples avoids relying on MC models for the estimate of the contribution of fake muons, thus reducing the large systematic uncertainties involved in hadronic background calculations. The residual SM background can be estimated from data using control regions thus reducing further potential systematic uncertainties of the simulation model.

The presented analysis allows to probe low mass mSUGRA region $m_0, m_{1/2} < 200$ GeV at $L_{acc} < 1$ fb^{-1} with LHC operating at *sqrts*=10 TeV.

References

[1] CDF, hep-exp/0808.2446, 2008.

[2] W deBoer et al., CMS-NOTE 2006/113, 2006.

[3] B.C. Allanach et al., hep-ph/0104145, Comput. Phys. Commun. 143 305-331, 2002.

[4] A. Djouadi et al., hep-ph/0609292v1.

[5] R. Barbieri et al., Phys. Lett. 119B 343, 1982.

[6] T. Sjostrand et al., hep-ph/0603175, 2006.

[7] J. Alwall et al., hep-ph/0706.2334, 2007.

[8] U. Baur et al., hep-ph/0211224, 2002.

[9] M. Mulders et al., CMS-AN 2008/098, 2008.

[10] S. Abdulin et al., hep-ph/0605143.

[11] RooStats https : //twiki.cern.ch/twiki/bin/view/RooStats/WebHome.